HOKKAIDO UNIVERSITY

Title	Hierarchy among viral RNA (vRNA) segments in their role in vRNA incorporation into influenza A virions
Author(s)	Muramoto, Yukiko; Takada, Ayato; Fujii, Ken; Noda, Takeshi; Iwatsuki-Horimoto, Kiyoko; Watanabe, Shinji; Horimoto, Taisuke; Kida, Hiroshi; Kawaoka, Yoshihiro
Citation	Journal of Virology, 80(5), 2318-2325 https://doi.org/10.1128/JVI.80.5.2318-2325.2006
Issue Date	2006-03
Doc URL	http://hdl.handle.net/2115/28152
Rights	Copyright © American Society for Microbiology.
Type	article
File Information	JV80-5.pdf

Hierarchy among Viral RNA (vRNA) Segments in Their Role in vRNA Incorporation into Influenza A Virions

Yukiko Muramoto,[1,2,3] Ayato Takada,[2,3] Ken Fujii,[2,3] Takeshi Noda,[3,4] Kiyoko Iwatsuki-Horimoto,[2,3] Shinji Watanabe,[5] Taisuke Horimoto,[2,3] Hiroshi Kida,[1] and Yoshihiro Kawaoka[2,3,4,5]*

Laboratory of Microbiology, Department of Disease Control, Graduate School of Veterinary Medicine, Hokkaido University, Sapporo 060-0818,[1] Division of Virology, Department of Microbiology and Immunology,[2] and International Research Center for Infectious Diseases,[4] Institute of Medical Science, University of Tokyo, Tokyo 108-8639, and Core Research for Evolutional Science and Technology, Japan Science and Technology Agency, Saitama 332-0012,[3] Japan, and Department of Pathobiological Sciences, School of Veterinary Medicine, University of Wisconsin—Madison, Madison, Wisconsin 53706[5]

The genome of influenza A viruses comprises eight negative-strand RNA segments. Although all eight segments must be present in cells for efficient viral replication, the mechanism(s) by which these viral RNA (vRNA) segments are incorporated into virions is not fully understood. We recently found that sequences at both ends of the coding regions of the HA, NA, and NS vRNA segments of A/WSN/33 play important roles in the incorporation of these vRNAs into virions. In order to similarly identify the regions of the PB2, PB1, and PA vRNAs of this strain that are critical for their incorporation, we generated a series of mutant vRNAs that possessed the green fluorescent protein gene flanked by portions of the coding and noncoding regions of the respective segments. For all three polymerase segments, deletions at the ends of their coding regions decreased their virion incorporation efficiencies. More importantly, these regions not only affected the incorporation of the segment in which they reside, but were also important for the incorporation of other segments. This effect was most prominent with the PB2 vRNA. These findings suggest a hierarchy among vRNA segments for virion incorporation and may imply intersegment association of vRNAs during virus assembly.

Viruses must retain their genomes during repeated cycles of replication. At a late stage of the infectious cycle, progeny viruses begin assembly into infectious virions by selecting their genomes from a large pool of viral and cellular nucleic acids. The regions important for the incorporation of a viral genome into virions are generally called packaging signals (10, 18, 29, 34). For example, the packaging signals of retroviruses, which are located in the 5′ end of the genome, interact with the Gag precursor, leading to the incorporation of the genome into virions (reviewed in reference 1). However, for many other viruses, the genomic packaging signals and the underlying packaging mechanisms remain unknown.

Influenza A virus is an enveloped negative-strand RNA virus. Its genome, which encodes up to 11 proteins, comprises eight viral RNA (vRNA) segments (PB2, PB1, PA, HA, NP, NA, M, and NS) (3, 17). The noncoding regions at the 3′ and 5′ termini of the eight vRNA segments contain highly conserved sequences that consist of 12 and 13 nucleotides, respectively. These sequences are partially complementary to allow the formation of a corkscrew structure (2, 5, 9, 14, 30) that constitutes the viral promoter for replication and transcription (28). Each vRNA segment interacts with viral nucleoprotein (NP) and three polymerase subunit proteins, PB2, PB1, and PA, to form viral ribonucleoprotein (vRNP) complexes, the minimal unit for transcription and replication of vRNAs. Newly synthesized vRNPs are exported from the nuclei of host cells to the plasma membrane, where they are incorporated into progeny virions. For influenza A viruses, only virions that possess all eight RNA segments can successfully complete viral replication. Hence, signals that ensure the incorporation of the viral genomic segments into virions must be present in the genome; however, the mechanism that drives vRNA virion incorporation is unknown.

When influenza viruses are passaged at a high multiplicity of infection, defective interfering virus particles, which contain defective RNAs with deletions in their coding regions, are produced (reviewed in reference 20). Defective RNAs are generated during vRNA replication, incorporated into virions, and maintained by coinfection with infectious viruses (8). Defective RNAs have been described for all eight influenza A virus segments (15, 24), although most are derived from the polymerase segments (i.e., PA, PB1, and PB2). These defective RNAs do not encode functional viral proteins, but they are retained in virus populations, indicating that they contain the structural features required for their incorporation into virions.

We recently found that, in addition to the noncoding regions (11), coding regions at both ends of the HA, NA, and NS vRNA segments play important roles in the incorporation of these segments into virions (11, 12, 33). These findings suggested that all influenza A virus segments possess segment-specific packaging signals for their efficient virion incorporation. We also found that the exclusion of a vRNA segment decreased the efficiency of infectious virion formation, even if the protein encoded by the omitted vRNA was supplied by a protein expression plasmid (12). These results suggested that

the vRNA segments per se play a role in the efficient formation of infectious virions.

Recently, Liang et al. (19) confirmed that, as with the segments we studied, both ends of the coding regions of PB2, PB1, and PA vRNAs are necessary for their efficient incorporation into virions. However, in their experiments, cells were transfected with plasmids for the expression of all eight wild-type vRNA segments, together with a plasmid expressing a test vRNA that comprised a reporter gene and a portion of one of the polymerase vRNA segments. Under these conditions, a test vRNA and its parent vRNA would compete for packaging into virions. This experimental approach complicates the analysis of the reporter vRNA incorporation efficiency and confounds interpretation of the data. We therefore took an alternative approach. We studied the incorporation of the polymerase vRNA segments under conditions in which the test vRNA did not have to compete with the parental wild-type RNA for virion incorporation, i.e., by providing seven wild-type vRNA segments and a test vRNA segment. Not only do these conditions more authentically mirror virus-infected cells, but they also allowed us to ask whether the regions important for the incorporation of a particular vRNA segment into virions also affect the virion incorporation efficiencies of the other vRNA segments.

MATERIALS AND METHODS

Cells and viruses. 293T human embryonic kidney cells were maintained in Dulbecco's modified Eagle's medium supplemented with 10% fetal calf serum and antibiotics. Madin-Darby canine kidney (MDCK) cells were grown in minimal essential medium (MEM) containing 10% newborn calf serum and antibiotics. After infection with influenza virus, the MDCK cells were maintained in MEM containing 0.3% bovine serum albumin (BSA). A/Puerto Rico/8/34 (PR8, H1N1) viruses were propagated in MDCK cells.

Reverse genetics. Reverse genetics was performed with plasmids that contain cDNAs of the A/WSN/33 (WSN, H1N1) viral genes between the human RNA polymerase I promoter and the mouse RNA polymerase I terminator (referred to as PolI plasmids) and eukaryotic protein expression plasmids under the control of the chicken β-actin promoter (16, 23), as described previously (21). Briefly, PolI plasmids and protein expression plasmids were mixed with the transfection reagent TransIT-293 (Mirus, Madison, WI), incubated at room temperature for 15 min, and added to 10^6 293T cells cultured in Opti-MEM I (Gibco-BRL). The total volume of the supernatant was adjusted to 1 ml. Forty-eight hours later, the supernatant containing infectious virus-like particles (VLPs) was harvested. In this study, the generated particles are unable to undergo multiple cycles of replication; hence, they will be referred to as VLPs.

Construction of plasmids. Plasmid pPolIPB2(0)GFP(0) allows the synthesis of a negative-sense vRNA comprising the 3′ noncoding region of the PB2 vRNA, the complementary coding sequence of enhanced green fluorescent protein (GFP) (Clontech), and the 5′ noncoding region of the PB2 vRNA. To generate this plasmid, we amplified pPolIPB2 (a plasmid for the production of wild-type PB2 vRNA [22]) by inverse PCR (26) using the back-to-back primers PB2-0-F (5′-CACACAGGTCTCAATAATGTCGAATAGTTTAAAAACGACCTTGTT TCTAC-3′) and PB2-0-R (5′-CACACAGGTCTCACCATATTGAATATAATT GACCTGCTTTCGCT-3′), both of which contain BsaI sites. The GFP gene was amplified by PCR with BbsI-containing primers. The two PCR fragments were incubated with the respective enzymes and ligated to produce pPolIPB2(0)GFP(0). Using the same strategy, we also generated a series of constructs that contained portions of the PB2 coding regions, in addition to the noncoding regions (see Fig. 2). These mutants were named according to the lengths of the coding region(s) they contained; PB2(120)GFP(30), for example, contains the 3′ PB2 noncoding region, 120 nucleotides that correspond to the coding sequence at the 3′ end of the vRNA, the GFP coding sequence, 30 nucleotides that correspond to the coding sequence at the 5′ end of the vRNA, and the 5′ PB2 noncoding region.

Similarly, a series of PB1 and PA plasmids were produced. For the PB1 segment, a plasmid for the production of wild-type PB1 vRNA (pPolIPB1) was amplified by inverse PCR using primers that contain BsmBI sites: PB1-120-F (5′-CACACACGTCTCAATAAGTTTCCAGAGCCCGAATTG-3′) and PB1-120-R (5′-CACACACGTCTCACCATCATGGTGTATCCTGTTCCTG-3′). For

the PA segment, we amplified pPolIPA, which produces wild-type PA vRNA, by inverse PCR with the following primers that contain BsmBI sites: PA-120-F (5′-CACACAGGTCTCAATAACCTGGGACCTTTGATCTTG-3′) and PA-120-R (5′-CACACAGGTCTCACCATAGTGCATATTGCTGCAAATTTGTTTG-3′). The PCR products were incubated with BsmBI and ligated with the GFP fragment to produce pPolIPB1(120)GFP(120) and pPolIPA(120)GFP(120), respectively. Deletion constructs were produced by employing the same strategy. All plasmid constructs were sequenced to ensure that unwanted mutations were not introduced by PCR.

Determination of the total number of VLPs and the number of VLPs containing test vRNAs (Fig. 1). 293T cells were transfected with a PolI plasmid transcribing a test vRNA derived from the PA, PB1, or PB2 vRNA, with plasmids for the transcription of the remaining seven vRNAs, and with plasmids for the expression of all 10 viral proteins. Forty-eight hours later, the supernatants were harvested, mixed with helper PR8 virus (multiplicity of infection, 0.1), and adsorbed to MDCK cells for 1 h at 37°C. The helper PR8 virus was included to provide functional polymerase proteins because the test vRNAs possessing the GFP gene do not encode these proteins. The MDCK cells were then washed with phosphate-buffered saline (PBS) and incubated with MEM for an additional 11 h.

Twelve hours postinfection, the numbers of cells expressing HA or NP protein and the reporter gene GFP were determined. To detect HA-positive cells, the cells were dispersed with a solution containing 0.025% trypsin and 0.02% EDTA and subsequently incubated in PBS containing 1% BSA and 0.1% sodium azide for 1 h on ice. After centrifugation, the cells were incubated for 1 h on ice with a
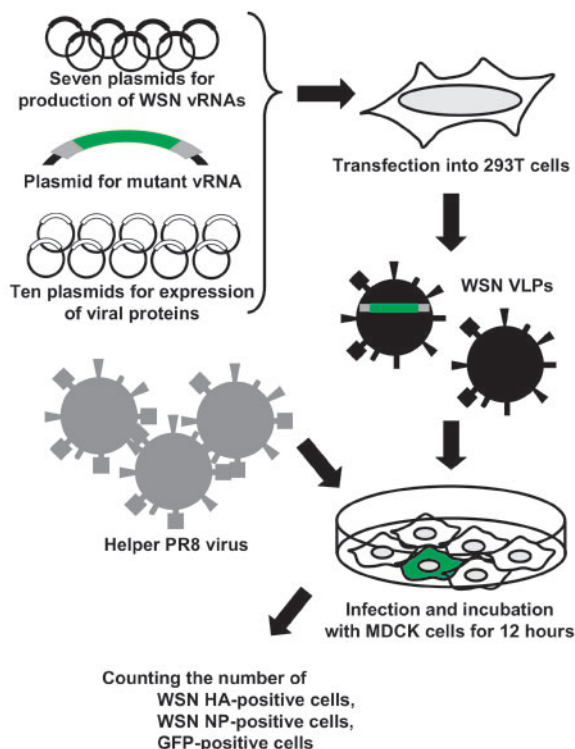

FIG. 1. Schematic representation of the system used to determine infectious virion formation and the incorporation efficiencies of test vRNA segments. 293T cells were transfected with plasmids for the production of WSN VLPs. Forty-eight hours later, the supernatants were mixed with helper PR8 virus and used to infect MDCK cells. At 12 h postinfection, the numbers of GFP- or WSN HA-positive cells were counted by flow cytometry; alternatively, the numbers of cells expressing WSN NP were determined. The number of cells expressing HA or NP was used to determine the number of infectious VLPs in the experiments presented in Table 1. The number of cells expressing GFP reflects the number of VLPs possessing a test vRNA. The incorporation efficiency of a test vRNA was determined by dividing the number of GFP-expressing cells by the sum of the number of cells expressing WSN HA and the number of GFP-expressing cells.

FIG. 2. Schematic diagram of mutant PB2 vRNAs and their efficiencies in virion formation and virion incorporation. The numbers of VLPs and the virion incorporation efficiencies of mutant PB2 vRNAs were determined by using the numbers of WSN HA- and GFP-expressing cells as a denominator. All mutants are shown in the negative-sense orientation. Each mutant contains the GFP reading frame (green bar); 27 and 34 nucleotides of the 3′ and 5′ noncoding regions, respectively (gray bars); and coding regions of various lengths (black bars). The dotted lines represent deleted sequences of the PB2 coding region. PB2(−) indicates the omission of this vRNA (i.e., VLPs were generated using only seven vRNA segments). The results shown are representative data from six independent experiments.

monoclonal antibody (967/8) that recognizes the WSN HA protein. The anti-HA mouse monoclonal antibody (967/8) reacted with the HA protein of WSN but not that of the PR8 virus (unpublished data). The cells were washed twice with PBS containing 0.1% sodium azide and incubated with a rhodamine-labeled goat anti-mouse immunoglobulin M (Chemicon, CA) for 1 h on ice. After two washes with sodium azide-containing PBS, the cells were resuspended in PBS. The GFP- and WSN HA-expressing cells were counted with a FACSCalibur cytometer (Becton Dickinson) according to standard procedures.

To detect WSN NP-positive cells, infected MDCK cells were treated with FACS Permeabilizing Solution (Becton Dickinson) for 10 min at room temperature and then incubated in PBS containing 1% BSA and 0.1% sodium azide. After incubation with an anti-NP monoclonal antibody (2S70/9) and rhodamine-labeled goat anti-mouse immunoglobulin G (Chemicon, CA), WSN NP-expressing cells were detected with the FACSCalibur cytometer. The anti-NP mouse monoclonal antibody (2S70/9) reacts with the NP protein of WSN virus, but not that of the helper PR8 virus (unpublished data).

Quantitative analysis of vRNAs in plasmid-transfected 293T cells. To ascertain the amounts of mutant vRNAs transcribed from the PolI plasmids in transfected cells, 293T cells were transfected with a plasmid for the transcription of a test vRNA, a plasmid for the transcription of an NS vRNA that is deficient in NS2 synthesis (32), plasmids for the transcription of the remaining six vRNAs, and protein expression plasmids for PB2, PB1, PA, and NP. The plasmid for the expression of a nonfunctional NS2 protein was used to prevent the production of virus capable of undergoing multiple cycles of replication. At 48 h posttransfection, total RNA was extracted with an RNeasy minikit (QIAGEN). To eliminate any residual transfected plasmid DNA, total RNA was treated with an RNase-Free DNase Set (QIAGEN) according to the manufacturer's instructions. The mutant vRNAs were reverse transcribed using TaqMan reverse transcription reagents (Applied Biosystems) with a strand-specific primer (available upon request) for the vRNA and then quantified using the ABI PRISM 7000 sequence detection system with primers (available upon request), TaqMan probes, and the TaqMan universal PCR master mix (Applied Biosystems).

RESULTS

A system to determine the virion incorporation efficiencies of PB2, PB1, and PA vRNAs. Most defective RNA segments of influenza A viruses retain 150 to 300 nucleotides corresponding to the 5′ and 3′ ends of the respective gene segment (7, 15, 24, 27), indicating that these 300 to 600 nucleotides likely possess the structural features required for efficient genome packaging. To identify the regions in the PB2, PB1, and PA vRNAs that are critical for vRNA virion incorporation and virion formation, we first generated plasmids in which the GFP gene is flanked by the noncoding regions and portions of the coding regions derived from both termini [PB2(300)GFP(300), PB1(300)GFP(300), and PA(120)GFP(120)] (outlined in Fig. 2, 3, and 4). Transfection of such a plasmid into 293T cells, together with expression plasmids for the PB2, PB1, PA, and NP proteins (minimal components for transcription and replication of vRNAs), resulted in the expression of GFP in cells (data not shown), indicating that the chimeric vRNAs were synthesized by the cellular RNA polymerase I and transcribed into mRNA by the viral proteins produced by the expression plasmids.

To calculate the vRNA virion incorporation efficiencies, the number of virions containing a test vRNA must be compared with the total number of VLPs. The total number of VLPs could be determined by inoculating cells with VLPs and then counting the number of cells expressing a given influenza virus protein. To

PB1 mutant vRNAs	Number of VLPs (/ml)	Number of VLPs possessing GFP vRNA (/ml)	Efficiency of virion incorporation
PB1(300)GFP(300)	93,000	60,800	65.4%
PB1(120)GFP(120)	134,800	84,000	62.3%
PB1(60)GFP(120)	113,600	67,200	59.2%
PB1(30)GFP(120)	58,800	27,400	46.6%
PB1(21)GFP(120)	125,200	78,200	62.5%
PB1(12)GFP(120)	121,000	70,800	58.5%
PB1(0)GFP(120)	34,200	0	0.0%
PB1(120)GFP(60)	55,000	38,000	69.1%
PB1(120)GFP(30)	44,600	23,800	53.4%
PB1(120)GFP(21)	68,000	26,200	38.5%
PB1(120)GFP(12)	26,800	16,200	60.4%
PB1(120)GFP(0)	19,400	0	0.0%
PB1(0)GFP(0)	42,000	400	1.0%
PB1(−) None	49,000	-	-

FIG. 3. Schematic diagram of mutant PB1 vRNAs and their efficiencies in virion formation and virion incorporation. Experiments were performed as outlined in the legend to Fig. 2. All mutants are shown in the negative-sense orientation. Each mutant contains the GFP sequence (green bar) flanked by 24 and 43 nucleotides of the 3′ and 5′ noncoding regions, respectively (gray bars), and coding regions of various lengths (black bars). PB1(−) indicates the omission of this vRNA. The results shown are representative data from three independent experiments.

ensure that the number of infectious VLPs determined by this method was not drastically affected by the viral gene product selected as a marker, we determined the number of cells expressing either HA or NP. Because we were testing the incorporation efficiencies of the PB2, PB1, and PA vRNAs, helper virus was needed to provide functional polymerase proteins. To distinguish between the HA and NP proteins expressed from our test VLPs (derived from WSN virus) and those expressed from the helper PR8 virus, we used antibodies that recognize the WSN HA and NP proteins, but not their PR8 virus counterparts.

To establish a system that allows us to assess the number of VLPs generated, we transfected 293T cells with a plasmid for the transcription of a test vRNA (derived from the PB2, PB1, or PA segment), 7 plasmids for the production of the remaining vRNAs, and 10 expression plasmids for the expression of the viral proteins (i.e., PB2, PB1, PA, HA, NP, NA, M1, M2, NS1, and NS2) (Fig. 1). Forty-eight hours later, VLP-containing supernatants derived from transfected cells were mixed with PR8 helper virus and used to infect MDCK

cells. Twelve hours postinfection, we determined the number of cells that expressed either HA or NP protein (Table 1). For all three vRNAs, the numbers of HA- or NP-expressing cells differed by less than a factor of 3; for example, using the PB2(300)GFP(300) test vRNA, we detected 240,800 HA-expressing cells versus 353,200 NP-expressing cells. Therefore, for the subsequent experiments, we determined the number of HA-expressing cells as an indicator of the efficiency of infectious virion formation. The incorporation efficiencies of test vRNAs were thus calculated by dividing the number of GFP-expressing cells (as a marker for the test vRNA) by the sum of the number of HA-expressing cells (as a marker for the number of virions) plus the number of GFP-expressing cells.

Sequences in the coding region of the PB2 vRNA affect infectious virion formation and vRNA virion incorporation. To delineate the sequences in the PB2 vRNA that are critical for virion formation and/or vRNA virion incorporation, we generated a series of plasmids for the production of PB2 vRNAs that express GFP and contain portions of the PB2 coding region

PA mutant vRNAs	Number of VLPs (/ml)	Number of VLPs possessing GFP vRNA (/ml)	Efficiency of virion incorporation
PA(120)GFP(120) 3' 24 120 GFP 120 58 5'	588,600	337,400	57.3%
PA(60)GFP(120) 60 120	661,000	368,800	55.8%
PA(30)GFP(120) 30 120	777,200	372,600	47.9%
PA(21)GFP(120) 21 120	1,285,600	806,600	62.7%
PA(12)GFP(120) 12 120	1,170,000	563,400	48.2%
PA(0)GFP(120) 120	284,400	70,000	24.6%
PA(120)GFP(60) 120 60	476,200	288,400	60.6%
PA(120)GFP(30) 120 30	734,600	479,000	65.2%
PA(120)GFP(21) 120 21	652,000	310,000	47.5%
PA(120)GFP(12) 120 12	142,000	40,400	28.5%
PA(120)GFP(0) 120	150,000	62,000	41.3%
PA(0)GFP(0)	143,000	8,000	5.6%
PA(-) None	87,400	-	-

FIG. 4. Schematic diagram of mutant PA vRNAs and their efficiencies in virion formation and virion incorporation. Experiments were performed as outlined in the legend to Fig. 2. All mutants are shown in the negative-sense orientation. Each mutant contains the GFP sequence (green bar) flanked by 24 and 58 nucleotides of the 3′ and 5′ noncoding regions, respectively (gray bars), and coding regions of various lengths (black bars). PA(−) indicates that this vRNA was omitted. The results shown are representative data from six independent experiments.

derived from both termini (Fig. 2), in addition to the noncoding regions of the PB2 vRNA (Fig. 2). The numbers of VLPs and the incorporation efficiencies of the test vRNAs were determined as described above.

First, we evaluated the efficiencies of infectious VLP production. With PB2(300)GFP(300), which contains 300 nucleotides corresponding to the 5′ and 3′ coding regions of the PB2 vRNA, we detected about 2.8×10^6 VLPs per ml (Fig. 2). Stepwise deletion of the coding sequences at the 3′ end of the vRNA (referred to as the 3′ coding region) had only moderate effects on the efficiency of VLP production; PB2(0)GFP(120), which lacks the entire coding region of the 3′ end, yielded about 1×10^6 VLPs/ml. Deletion of the coding sequences at the 5′ end of the vRNA (referred to as the 5′ coding region) [PB2(120)GFP(0)], however, reduced VLP production by 98% of that of PB2(300)GFP(300) and yielded a number of VLPs comparable to that obtained in the absence of the PB2 vRNA [PB2(−)]. This result suggests that sequences in the 5′ coding region of the PB2 vRNA are critical for the efficient generation of infectious virions. Further analysis revealed that 30 nucleotides of the 5′ coding region are critical for this effect

[compare the numbers of VLPs for PB2(120)GFP(0) and PB2(120)GFP(30)].

We next focused on the efficiencies of vRNA virion incorporation and found that for PB2(300)GFP(300), 54.7% of the VLPs contained the PB2(300)GFP(300) test vRNA, indicating that the 300 terminal nucleotides at both ends are sufficient for virion incorporation. To achieve the incorporation efficiencies observed for wild-type segments, internal PB2 coding sequences would likely be required. Stepwise deletion of nucleotides in the 3′ coding region of the PB2 vRNA had only moderate effects provided 30 or more nucleotides were retained; the deletion of these remaining 30 nucleotides, however, reduced the virion incorporation efficiency to 29.5% for PB2(0)GFP(120), demonstrating that this region is important for the efficient incorporation of the PB2 vRNA into virions. For PB2 vRNAs that lack a functional packaging sequence in the 3′ coding region, sequences in the 5′ coding region do contribute to virion incorporation, as exemplified by the inability of the PB2(0)GFP(0) test vRNA to be incorporated.

Deletions in the 5′ coding region only, by contrast, had no effect on incorporation efficiencies, as demonstrated by a 75.7%

TABLE 1. Contributions of individual vRNAs
to infectious virion production[a]

Mutant vRNA	No. of VLPs (VLPs/ml) detected by counting:	
	WSN HA-expressing cells[b]	WSN NP-expressing cells[b]
PB2(300)GFP(300)	240,800	353,200
PB2(0)GFP(0)	9,400	16,200
PB2(−)[c]	3,800	11,200
PB1(300)GFP(300)	332,000	292,400
PB1(0)GFP(0)	307,200	147,400
PB1(−)[c]	148,800	108,000
PA(120)GFP(120)	71,000	88,600
PA(0)GFP(0)	23,800	33,200
PA(−)[c]	24,800	24,600
HA(468)GFP(513)	NA	64,000
HA(0)GFP(0)	NA	33,600
HA(−)[c]	NA	27,400
NP(300)GFP(300)	36,600	NA
NP(0)GFP(0)	23,000	NA
NP(−)[c]	21,600	NA
NA(183)GFP(157)	21,600	13,600
NA(0)GFP(0)	15,600	21,600
NA(−)[c]	16,000	15,000
M(222)GFP(220)	24,600	44,600
M(0)GFP(0)	4,200	28,600
M(−)[c]	6,600	22,800
NS(150)GFP(150)	659,400	591,000
NS(0)GFP(0)	214,400	195,800
NS(−)[c]	129,000	122,800

[a] A plasmid for the production of a mutant vRNA and those for the remaining seven authentic WSN vRNAs were transfected into 293T cells, along with protein expression plasmids. VLPs produced from the cells were inoculated into MDCK cells, together with a helper PR8 virus. The efficiency of VLP generation can fluctuate due to subtle differences in experimental conditions. However, the tendencies observed in the efficiency of VLP generation among the test constructs are consistent. Therefore, the results shown are representative data from three independent experiments.

[b] The numbers of VLPs were determined by counting the WSN HA- or NP-expressing cells by flow cytometry. NA, not applicable.

[c] The vRNA was omitted; that is, VLPs were generated in the presence of only seven vRNA segments.

incorporation rate for PB2(120)GFP(0). Thus, while the use of this test vRNA produced a very low number of infectious VLPs, the test vRNA was efficiently incorporated into these particles. This finding suggests that sequences in the PB2 vRNA are involved in two biologically distinct processes: efficient infectious virion formation (a function residing in the 5′ coding region) and efficient vRNA incorporation into particles (a function primarily residing in the 3′ coding region).

The differences in packaging efficiencies could reflect differences in transcription levels of the test vRNAs in 293T cells. To exclude this possibility, we examined the levels of PB2(0)GFP(0) and PB2(120)GFP(120) in plasmid-transfected 293T cells using real-time PCR. The amount of PB2(0)GFP(0) vRNA was 52% of that of PB2(120)GFP(120); however, this difference is unlikely to explain the 99% reduction in VLP generation and the abrogation of vRNA virion incorporation.

The coding regions in the PB1 and PA vRNAs are also required for infectious virion formation and incorporation into virions. Next, we carried out similar experiments for the PB1 and PA vRNAs (Fig. 3 and 4). For the PB1 segment, deletion of the 3′ coding region only [PB1(0)GFP(120)], the 5′ coding region only [PB1(120)GFP(0)], or both coding regions [PB1(0)GFP(0)] reduced the efficiencies of virion formation

(Fig. 3), suggesting that sequences at both ends of this vRNA are required for efficient infectious virion formation; the 3- to 7-fold drop in efficiency, however, was much more moderate than the 100-fold reduction observed with some of the PB2 vRNA deletion constructs. We observed a similar pattern for the PA test vRNAs (Fig. 4), in which deletion of the 3′ coding region only [PA(0)GFP(120)], deletions in the 5′ coding region that retained 12 or fewer nucleotides [PA(120)GFP(12) and PA(120)GFP (0)], or deletion of both coding regions [PA(0) GFP(0)] affected the efficiencies of virion formation; the effect, however, was less pronounced than that observed with the PB2 vRNA.

With regard to vRNA virion incorporation efficiencies, we found that for the PB1 segment, 12 nucleotides in the 3′ coding region [PB1(12)GFP(120)] and 12 nucleotides in the 5′ coding region [PB1(120)GFP(12)] were sufficient for efficient incorporation of the respective test vRNAs (Fig. 3), while the deletion of these nucleotides [PB1(0)GFP(120)] and [PB1(120)GFP(0)] abrogated the incorporation of the respective vRNAs into virions. Hence, both ends of the vRNA harbor incorporation signals that seem to act independently and that cannot compensate for each other. For the PA segment, the deletion of sequences in either the 3′ or 5′ coding region affected the incorporation efficiencies only moderately (Fig. 4), while the deletion of both noncoding regions [PA(0) GFP(0)] had a significant effect, suggesting that the synergistic functions of the sequences at both ends of the viral RNA are required for efficient virion incorporation.

To exclude the possibility that differences in transcription levels accounted for the reduced efficiencies of virion formation and/or vRNA virion incorporation, we again determined the amounts of selected test vRNA in plasmid-transfected cells. The amount of PB1(0)GFP(0) was 37.8% of that of PB1(120)GFP(120), while the amount of PA(0)GFP(0) was 30.9% of that of PA(120)GFP(120). As was the case with the PB2 vRNA, these differences are unlikely to explain the differences observed in VLP formation and/or vRNA incorporation.

Hierarchy among vRNA segments in their roles in the incorporation of other vRNAs into virions. Our data suggested that the PB2 vRNA is more critical for efficient infectious virion generation than the PB1 or PA vRNA. We therefore speculated that a hierarchy exists in which the PB2 vRNA is critical for the efficient virion incorporation of other vRNAs, while the omission of other segments is tolerable to some extent. To test this possibility, we examined the effects of both ends of the coding regions in all eight vRNAs on infectious virion formation. For each segment, two test vRNAs were used that either lacked the entire coding sequence or contained sequences from both ends of the coding regions that have been shown by us to allow efficient incorporation (Table 1) [the NA, HA, and NS constructs are described in references 11, 12, and 33; M(0)GFP (0) and M(222)GFP(220), M. Ozawa, J. Maeda, and Y. Kawaoka, unpublished data; NP(0)GFP(0) and NP(300)GFP (300), M. Ozawa and Y. Kawaoka, unpublished data]. We also tested infectious virion formation in the absence of each of the eight vRNA segments. The number of infectious VLPs was determined by counting the number of HA- or NP-expressing cells.

For the majority of the segments, the total numbers of virions differed by less than a factor of 2 for the two detection

systems (i.e., detection of HA- or NP-expressing cells), allowing us to reliably detect overall trends for the efficiency of infectious virion formation. Overall, mutant vRNAs lacking the entire coding region reduced the efficiencies of infectious virion formation compared to the respective vRNAs possessing sequences derived from both the 5′ and 3′ coding regions; the noticeable exception was the NA segment when the number of infectious virions was determined by counting NP-positive cells. In addition, for some vRNA segments, the number of VLPs produced with only seven vRNAs was further reduced compared to the number produced with the test vRNAs that lacked the coding region (Table 1). Most importantly, however, the effects on the efficiency of virion formation differed among the different vRNA segments. Omission of the PB2 vRNA resulted in an ~30-fold reduction in VLP production, whereas omission of the other vRNA segments resulted in 1.4- to 5.1-fold reductions. These results provided further proof of a hierarchy among the vRNA segments with respect to the importance of the individual vRNAs for the incorporation of the other vRNA segments.

To study the contributions of the polymerase and NP vRNAs to virion formation, we had to include a helper virus to provide the corresponding proteins. To ensure comparable experimental conditions, we also used helper virus for the experiments involving the HA, NA, M, and NS vRNA segments, although it could have been omitted for these gene segments. To exclude the possibility that the efficiency of virion formation was affected by the helper virus, the efficiencies of virion formation for mutant HA, NA, M, and NS vRNAs were examined in the absence of helper virus. The results were essentially the same as those shown in Table 1 (data not shown). Therefore, the use of helper virus did not affect the results.

DISCUSSION

Here, we demonstrated that sequences in the coding region of the PB2 vRNA segment of WSN have a dramatic effect on the efficiency of infectious virion formation, as measured by HA- and NP-expressing cells. Although deletions in the coding regions of other vRNA segments also affected the efficiencies of infectious virion formation, these effects were much less dramatic. The PB2 vRNA may, therefore, perform a primary role in the incorporation of other vRNAs into virions.

How do the sequences at the ends of the coding regions of vRNAs contribute to the efficiency of infectious virion formation? In this study, the number of infectious virions was determined by counting HA-expressing cells (when testing for vRNAs other than HA) or NP-expressing cells (when testing for vRNAs other than NP); hence, we examined the effect of a test vRNA on the incorporation of HA or NP vRNA into virions. Our results imply that the truncation of a coding region of a vRNA segment reduces the incorporation efficiencies of the other vRNAs; that is, for all eight individual vRNAs, their coding regions may be required for the efficient virion incorporation of the other vRNA segments. Thus, prior to or at the time of genome incorporation into virions, vRNA segments (as a form of vRNPs) may come together. Indeed, electron microscopy of influenza A virus has revealed that budding virions contain eight RNP molecules (25), indicating that the RNPs

likely assemble to form a multisegmented macromolecule consisting of eight RNPs. In retroviruses, genomic RNAs always form dimers in mature virions. Two RNA molecules are linked at the dimer initiation site/dimer linkage sequence (4, 13), which overlaps with the packaging signal. This dimerization of RNA is thought to be important for genome incorporation into virions (31). By analogy, the ends of the coding regions in influenza virus RNAs may serve not only as packaging signals, but also as "linkage sites" that facilitate interactions with other vRNAs. Thus, influenza virus vRNA segments may form a multisegmented macromolecule through these linkage sites by direct or indirect interactions with other vRNA segments. The finding that one segment can affect the incorporation of other segments is consistent with this linkage model. The devastating effect on the incorporation of other vRNA segments suggests a critical role for PB2 vRNA in this process and possibly in the formation of the multisegmented macromolecule. Electron microscopic studies revealed structures in which a center "dot," most likely a vRNP complex, is surrounded by seven dots (25). Based on this finding, one might envision a scenario in which the PB2 vRNA occupies the center position around which the other vRNAs assemble; omission of this center piece may have a more significant effect on the formation of the vRNP structures than the omission of any of the other vRNPs. Likewise, the deletion of the 5′ coding region may abrogate the interaction with the other vRNAs and thus the efficient formation of infectious VLPs. Further studies of the hierarchy among vRNA segments are in progress and should increase our understanding of the mechanism of influenza virus genome packaging.

As previously determined for the HA (33), NA (12), and NS (11) segments, our data indicate that the sequences required for efficient virion incorporation of the PB2, PB1, and PA vRNAs reside in the coding regions. Recently, Dos Santos Afonso et al. also showed that both ends of the coding region of PB2 vRNA were needed for efficient incorporation of the PB2 vRNA in infectious virus (6). Preliminary studies for the remaining NP (Ozawa and Kawaoka, unpublished) and M (Ozawa et al., unpublished) segments produced similar results. Thus, for all eight vRNA segments of influenza A viruses, the ends of the coding regions play important roles in vRNA virion incorporation, although the relative contributions of the 3′ and 5′ ends differ among the vRNA segments. For the NS vRNA, we have further shown that segment-specific noncoding regions are also required for efficient virion incorporation (11). This finding may extend to the other vRNA segments. During the preparation of our manuscript, Liang et al. (19) reported that the 5′-terminal coding region of the PB2 vRNA is more important than the 3′-end coding region for virion incorporation, similar to results previously published by Duhaut and Dimmock (8). Although we agree with Liang et al. (19) that the 5′ coding region contributes to this process, we found that the 3′ end of the PB2 vRNA is more important for efficient virion incorporation. This discrepancy may reflect differences in our assay systems; that is, we evaluated virion incorporation of test vRNA segments in the absence of corresponding authentic vRNA segments, whereas Liang et al. (19) assessed the incorporation of their test vRNAs into virions in the presence of the corresponding authentic vRNA. This competition between the test and the authentic vRNAs for virion incorporation may account for the observed differences.

The precise mechanism by which the packaging signals of different vRNA segments affect their incorporation into virions remains unknown. In influenza virus RNAs, the sequences at the 3′- and 5′-terminal noncoding regions are partially complementary and form a corkscrew structure (2, 5, 9, 14, 30). Although the regions that are important for vRNA virion incorporation are not in immediate proximity, the two structures may be close to each other in the vRNP tertiary structure. It may, therefore, be the tertiary structure, formed by both ends of the coding regions, together with segment-specific noncoding regions, that is recognized by viral components and/or host cell factors as part of the requirements for vRNA incorporation into virions.

REFERENCES

1. **Berkowitz, R., J. Fisher, and S. P. Goff.** 1996. RNA packaging. Curr. Top. Microbiol. Immunol. **214:**177–218.
2. **Catchpole, A. P., L. J. Mingay, E. Fodor, and G. G. Brownlee.** 2003. Alternative base pairs attenuate influenza A virus when introduced into the duplex region of the conserved viral RNA promoter of either the NS or the PA gene. J. Gen. Virol. **84:**507–515.
3. **Chen, W., P. A. Calvo, D. Malide, J. Gibbs, U. Schubert, I. Bacik, S. Basta, R. O'Neill, J. Schickli, P. Palese, P. Henklein, J. R. Bennink, and J. W. Yewdell.** 2001. A novel influenza A virus mitochondrial protein that induces cell death. Nat. Med. **7:**1306–1312.
4. **Coffin, J.** 1984. Genome structure, p. 261–368. *In* R. Weiss, N. Teich, H. Vermus, and J. Coffin (ed.), RNA tumor viruses. Cold Spring Harbor Laboratory Press, Cold Spring Harbor, N.Y.
5. **Desselberger, U., V. R. Racaniello, J. J. Zazra, and P. Palese.** 1980. The 3′ and 5′-terminal sequences of influenza A, B and C virus RNA segments are highly conserved and show partial inverted complementarity. Gene **8:**315–328.
6. **Dos Santos Afonso, E., N. Escriou, I. Leclercq, S. van der Werf, and N. Naffakh.** 2005. The generation of recombinant influenza A viruses expressing a PB2 fusion protein requires the conservation of a packaging signal overlapping the coding and noncoding regions at the 5′ end of the PB2 segment. Virology **341:**34–46.
7. **Duhaut, S. D., and N. J. Dimmock.** 1998. Heterologous protection of mice from a lethal human H1N1 influenza A virus infection by H3N8 equine defective interfering virus: comparison of defective RNA sequences isolated from the DI inoculum and mouse lung. Virology **248:**241–253.
8. **Duhaut, S. D., and N. J. Dimmock.** 2000. Approximately 150 nucleotides from the 5′ end of an influenza A segment 1 defective virion RNA are needed for genome stability during passage of defective virus in infected cells. Virology **275:**278–285.
9. **Flick, R., and G. Hobom.** 1999. Interaction of influenza virus polymerase with viral RNA in the 'corkscrew' conformation. J. Gen. Virol. **80:**2565–2572.
10. **Fosmire, J. A., K. Hwang, and S. Makino.** 1992. Identification and characterization of a coronavirus packaging signal. J. Virol. **66:**3522–3530.
11. **Fujii, K., Y. Fujii, T. Noda, Y. Muramoto, T. Watanabe, A. Takada, H. Goto, T. Horimoto, and Y. Kawaoka.** 2005. Importance of both the coding and the segment-specific noncoding regions of the influenza A virus NS segment for its efficient incorporation into virions. J. Virol. **79:**3766–3774.
12. **Fujii, Y., H. Goto, T. Watanabe, T. Yoshida, and Y. Kawaoka.** 2003. Selective incorporation of influenza virus RNA segments into virions. Proc. Natl. Acad. Sci. USA **100:**2002–2007.
13. **Greatorex, J., and A. Lever.** 1998. Retroviral RNA dimer linkage. J. Gen. Virol. **79:**2877–2882.
14. **Hsu, M. T., J. D. Parvin, S. Gupta, M. Krystal, and P. Palese.** 1987. Genomic RNAs of influenza viruses are held in a circular conformation in virions and in infected cells by a terminal panhandle. Proc. Natl. Acad. Sci. USA **84:** 8140–8144.
15. **Jennings, P. A., J. T. Finch, G. Winter, and J. S. Robertson.** 1983. Does the higher order structure of the influenza virus ribonucleoprotein guide sequence rearrangements in influenza viral RNA? Cell **34:**619–627.
16. **Kobasa, D., M. E. Rodgers, K. Wells, and Y. Kawaoka.** 1997. Neuraminidase hemadsorption activity, conserved in avian influenza A viruses, does not influence viral replication in ducks. J. Virol. **71:**6706–6713.
17. **Lamb, R. A., and R. M. Krug.** 2001. Orthomyxoviridae: the viruses and their replication, p. 1487–1531. *In* D. M. Knipe and P. M. Howley (ed.), Fields virology, 4th ed. Lippincott-Raven Publishers, Philadelphia, Pa.
18. **Lever, A., H. Gottlinger, W. Haseltine, and J. Sodroski.** 1989. Identification of a sequence required for efficient packaging of human immunodeficiency virus type 1 RNA into virions. J. Virol. **63:**4085–4087.
19. **Liang, Y., Y. Hong, and T. G. Parslow.** 2005. *cis*-acting packaging signals in the influenza virus PB1, PB2, and PA genomic RNA segments. J. Virol. **79:**10348–10355.
20. **Nayak, D. P., T. M. Chambers, and R. K. Akkina.** 1985. Defective-interfering (DI) RNAs of influenza viruses: origin, structure, expression, and interference. Curr. Top. Microbiol. Immunol. **114:**103–151.
21. **Neumann, G., T. Watanabe, H. Ito, S. Watanabe, H. Goto, P. Gao, M. Hughes, D. R. Perez, R. Donis, E. Hoffmann, G. Hobom, and Y. Kawaoka.** 1999. Generation of influenza A viruses entirely from cloned cDNAs. Proc. Natl. Acad. Sci. USA **96:**9345–9350.
22. **Neumann, G., T. Watanabe, and Y. Kawaoka.** 2000. Plasmid-driven formation of influenza virus-like particles. J. Virol. **74:**547–551.
23. **Niwa, H., K. Yamamura, and J. Miyazaki.** 1991. Efficient selection for high-expression transfectants with a novel eukaryotic vector. Gene **108:**193–199.
24. **Noble, S., and N. J. Dimmock.** 1995. Characterization of putative defective interfering (DI) A/WSN RNAs isolated from the lungs of mice protected from an otherwise lethal respiratory infection with influenza virus A/WSN (H1N1): a subset of the inoculum DI RNAs. Virology **210:**9–19.
25. **Noda, T., H. Sagara, A. Yen, A. Takada, H. Kida, R. H. Cheng, and Y. Kawaoka.** Architecture of ribonucleoprotein complexes in influenza A virus particles. Nature, in press.
26. **Ochman, H., A. S. Gerber, and D. L. Hartl.** 1988. Genetic applications of an inverse polymerase chain reaction. Genetics **120:**621–623.
27. **Odagiri, T., and M. K. Tobita.** 1990. Mutation in NS2, a nonstructural protein of influenza A virus, extragenically causes aberrant replication and expression of the PA gene and leads to generation of defective interfering particles. Proc. Natl. Acad. Sci. USA **87:**5988–5992.
28. **Parvin, J. D., P. Palese, A. Honda, A. Ishihama, and M. Krystal.** 1989. Promoter analysis of influenza virus RNA polymerase. J. Virol. **63:**5142–5152.
29. **Pollack, J. R., and D. Ganem.** 1993. An RNA stem-loop structure directs hepatitis B virus genomic RNA encapsidation. J. Virol. **67:**3254–3263.
30. **Robertson, J. S.** 1979. 5′ and 3′ terminal nucleotide sequences of the RNA genome segments of influenza virus. Nucleic Acids Res. **6:**3745–3757.
31. **Sakuragi, J., S. Ueda, A. Iwamoto, and T. Shioda.** 2003. Possible role of dimerization in human immunodeficiency virus type 1 genome RNA packaging. J. Virol. **77:**4060–4069.
32. **Watanabe, T., S. Watanabe, G. Neumann, H. Kida, and Y. Kawaoka.** 2002. Immunogenicity and protective efficacy of replication-incompetent influenza virus-like particles. J. Virol. **76:**767–773.
33. **Watanabe, T., S. Watanabe, T. Noda, Y. Fujii, and Y. Kawaoka.** 2003. Exploitation of nucleic acid packaging signals to generate a novel influenza virus-based vector stably expressing two foreign genes. J. Virol. **77:**10575–10583.
34. **Weiss, B., H. Nitschko, I. Ghattas, R. Wright, and S. Schlesinger.** 1989. Evidence for specificity in the encapsidation of Sindbis virus RNAs. J. Virol. **63:**5310–5318.